

Physical Characterization of Poly (vinyl pyrrolidone) and Gelatin Blend Films Doped with Magnesium Chloride

E. M. Abdelrazek^a, H.M. Ragab^b, M. Abdelaziz^{a,c*}

^aPhysics Department, Faculty of Science, Mansoura University, Mansoura, Egypt

^b Physics Department, Faculty of Science, Al-Azhar University (Girls), Egypt

^cNatural Science Department, Community College of Riyadh, King Saud University, kingdom of Saudi Arabia

^aemabdelrazek@yahoo.com; ^{a,c*}mabdelaziz62@yahoo.com

Abstract

Polymeric films of pure poly (vinyl pyrrolidone) (PVP) and PVP/gelatin blend (60/40) containing various amounts of $MgCl_2$ were prepared using a casting technique. The structural and related physical properties of the prepared films were studied using different techniques. The obtained data revealed that the addition of gelatin and magnesium chloride causes structural variation in the PVP network. The X-Ray diffraction (XRD) patterns reveal that the amorphous nature of the blend increases with the concentration of magnesium chloride. Complex formation was confirmed by XRD and FT-IR analysis. The DSC results indicate that the addition of both gelatin and magnesium chloride to PVP changes the thermal behavior, such as the glass transition temperature and thermal stability. The analysis of the UV-visible optical absorption shows the decrease in the optical band gap (E_g) as dopant concentration increase. The reduced values of the optical gap improve their optical response, which can be used as optical sensors. The direct current (DC) electrical resistivity studies revealed a linear temperature dependence of the hopping distance (R_0) for all doped films. The conduction mechanism discussed based on the phonon-assisted charge carrier inter-polaron hopping model. Moreover, the addition of both gelatin and $MgCl_2$ gives rise to improve the electrical properties of PVP film. The optical and electrical results suggested the applicability of these materials in optical and/or electrical sensors.

Keywords

Blends; XRD; FT-IR; DSC; Optical; Electrical Properties

Introduction

Polymer science has shown a tendency in the last decade to create blends of different polymers rather than to develop new polymers. Blending of polymers is one of the simplest means to obtain a variety of physical and chemical properties from the constituent polymers. The gain in newer properties depends on

the degree of compatibility or miscibility of the polymers at a molecular level. Generally, the polymer-polymer miscibility is due to some specific interactions like dipole-dipole forces, hydrogen bonding and charge transfer complexes between the polymer segments.

Water soluble polymers are important from industrial view point. Polyvinyl pyrrolidone (PVP) has excellent characteristics such as high-dielectric constant, dissolubility, stability, compatibility and resistance and large scale screen printing of PVP films at low cost is feasible. PVP is highly soluble in polar solvents such as alcohol, so it is preferable to avoid phase separation in the reaction. Another advantage of using PVP is that PVP can be thermally crosslinked and that makes the composites have outstanding thermal stability and high mechanical strength. Furthermore, the amorphous structure of PVP also provides a low scattering loss, which makes it an ideal polymer for composite materials for optical application. PVP thermally decompose before reaching its molten state. This terminates the application of this polymer. PVP is chosen as a matrix for the composites because of the two important characteristics. One is that PVP has good film-forming and adhesive behavior on many solid substrates and its films exhibit good optical quality and mechanical strength. Another is that the pyrrolidone group of PVP prefers to complex with many inorganic salts resulting in fine dispersion and surface passivation of them. Blending PVP with a potentially useful natural biopolymer such as gelatin seems to be an interesting way of preparing a polymeric composite. Gelatin not only maintains inherent biological activities of PVP, but also gains a lot of new properties and functions. Such a composite

reported improved thermal stability and absorbability when used as matrices for magnesium chloride. As aforementioned, several researchers have reported of PVP and its blends with other polymers. However, there is little research reported on the preparation and physical characterization of PVP and gelatin blend doped with metal halide.

The present work is carried out to investigate the effect of both doping gelatin and magnesium chloride on the structure of PVP using XRD, FT-IR and DSC techniques. These composites obtained would offer opportunities to explore their novel optical, thermal and electronic properties.

Experimental work

Sample preparation

Poly (vinyl pyrrolidone) (PVP) from Aldrich chemical co. Ltd England were used as received. The quantity of PVP and gelatin (60/40) by weight to weight (wt %) was added to doubly distilled water with stirring the solution at 343K to complete dissolution. Required quantity (0.0, 2, 6, 8, 10, 15 and 20 wt%) of MgCl_2 was also dissolved in doubly distilled water and added to the polymeric solution with continuous stirring. Then the solution was left for 24 hour to eliminate bubbles. The solution was poured onto cleaned Petri dishes and dried in oven at 333 K for 4 days to ensure removal of the solvent traces. After drying, the films were peeled from Petri dishes and kept in vacuum desiccators until use. The thickness of the obtained films was in the range of $\approx 80\text{--}90\ \mu\text{m}$ for the FT-IR measurement and $100\text{--}150\ \mu\text{m}$ for other measurements.

Measuring techniques

The X-Ray diffraction (XRD) scans were obtained using a Seimens type F diffractometer with $\text{CuK}\alpha$ radiation and LiF monochromator. FT-IR absorption spectra were carried out using the single beam Fourier transform-infrared spectrometer (FT-IR-430, JASCO, Japan). FT-IR spectra of the samples were obtained in the spectral range of $4000\text{--}400\ \text{cm}^{-1}$. The differential scanning calorimetry (DSC) measurements were performed by using a Shimadzu DSC-50 apparatus in the temperature range $303\text{--}873\ \text{K}$ with a heating rate of $10\ \text{K/min}$. Ultraviolet and visible (UV-VIS) absorption spectra were measured in the wavelength region of $200\text{--}900\ \text{nm}$ using spectrophotometer (V-570 UV/VIS/NIR, JASCO, Japan). The direct current electrical resistivity was measured using an auto-range multimeter (Keithley 175) with an accuracy of $\pm 2\%$.

Results and discussion

X-Ray diffraction (XRD)

The measured XRD profiles of pure PVP, PVP/gelatin blend, PVP/gelatin: MgCl_2 films and MgCl_2 are shown in FIG. 1. There was a noticeable change in the intensity of XRD peaks of the doped samples in addition to appearance of additional peaks. The pure PVP scan shows very broad diffraction peak around $2\theta = 22.3^\circ$, which confirms the amorphous nature of the prepared polymer film that is conformity with either reported in literature. When gelatin was added into PVP, making PVP/gelatin blend, the intensity of this peak increased and became sharper. An increase in the intensity and decrease in the width of PVP/gelatin blend are observed indicating a semicrystalline structure, which leads to their good compatibility. Similar result was reported by Nagahama et al. For the addition of MgCl_2 to the blend matrix, there is a shift in the diffraction peak towards lower diffraction angles confirmed a complex formation. Moreover, there is a scattering peak at $2\theta = 8.5^\circ$ was observed for doping levels 10 and 20 wt%. This peak belongs neither to PVP nor PVP/gelatin or MgCl_2 . This peak may indicate the appearance of new crystalline phase of the blend matrix. Furthermore, the peaks for $2\theta = 21.5^\circ, 23^\circ, 29^\circ$ and 36° , pertaining to MgCl_2 disappeared in the complexes which indicate the complete dissociation of the salt in the polymer matrix. This observation confirms that complexation has taken place in the amorphous phase. The decrease in the intensities of the peaks on doping shows that the decrease in the crystallinity and simultaneous increase in the amorphousity of the complexed films. This amorphous nature is responsible for greater ionic diffusivity resulting in high ionic conductivity.

Fourier transforms infrared analysis

FIG. 2 shows the FT-IR spectra of PVP/gelatin blend film as well as PVP/gelatin: MgCl_2 films in the range of $2000\text{--}400\ \text{cm}^{-1}$. Both the spectrum of PVP, not shown, and PVP/gelatin films have nearly similar characteristic FTIR bands. Spectrum of the blend film shows intense peaks at $1661, 1466$ and $1285\ \text{cm}^{-1}$ corresponding to C=O , C=C and C=N respectively. A broad peak located at $918\ \text{cm}^{-1}$ is due to the outer face vibration oscillation of the hydroxyl group ($\delta_{\text{O-H}}$). The other peaks centered at 1425 and $1285\ \text{cm}^{-1}$ are assigned to the inner face bending vibrations of the hydroxyl group. The spectra of PVP/gelatin: MgCl_2 films show some difference as follows;

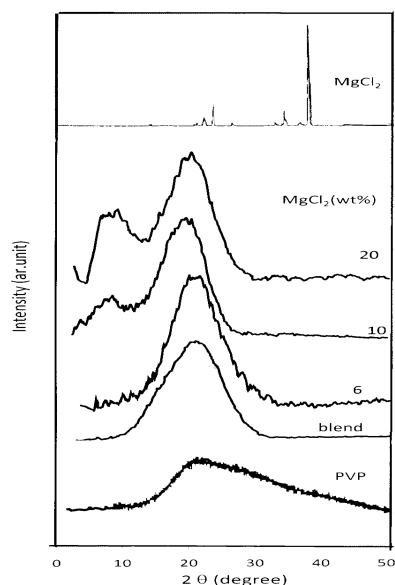


FIG.1 XRD PATTERNS OF PURE PVP, PVP/GELATIN BLEND, PVP/GELATIN BLEND DOPED WITH (6, 10 AND 20 WT%) OF MgCl_2 AND MgCl_2 SALT

- 1) The increasing in the intensity and shifting towards higher wavenumber of the absorption peak at about 627 cm^{-1} , assigned to Mg-O-Mg stretching, corresponded to strong interaction between polymer matrix and dopant.

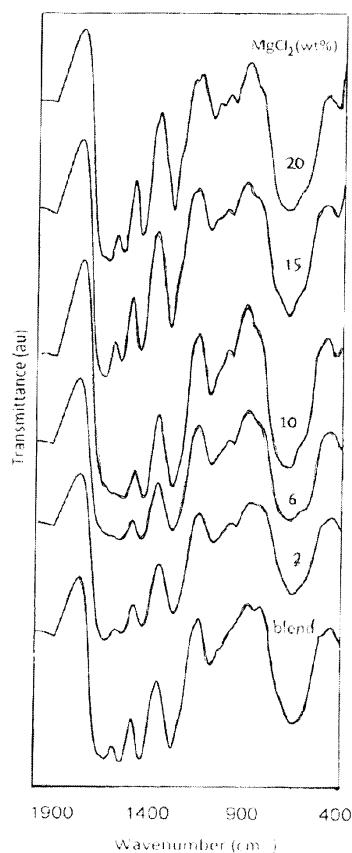


FIG. 2 FT-IR ABSORPTION SPECTRA OF PURE PVP/GELATIN BLEND AND PVP/GELATIN BLEND DOPED WITH MgCl_2

- 2) New absorption bands in between 700 to 900 cm^{-1} are observed. The new bands may be correlated likewise to defects induced by the charge transfer reaction between the polymer chain and the dopant.
- 3) Shift of peak from 1617 cm^{-1} to 1661 cm^{-1} , indicated strong coulombic interaction between PVP and Mg ions. Some researchers have proposed that the shifting of the C = O group in PVP can be attributed to the charge of p- π conjugation associated with the amide group of PVP arising from dissociation of PVP chains due to the incorporation of other species. It is possible that the interaction between the dopant and PVP leads to the dissociations of the aggregated PVP chains, resulting in the shifting of the C=O vibration band. From the summarized spectra features listed above, it can be seen that stronger molecular interaction exists between polymers and dopant.

Differential scanning calorimetry

The thermal properties of pure PVP as well as PVP/gelatin blend and their complexed films were examined by DSC to estimate how the thermal transitions of the prepared films were affected by the different concentrations of MgCl_2 as shown in FIG. 3. For pure phase of PVP, FIG. 3, the curve of DSC shows a major endothermic peak centered at about $T_g = 345\text{ K}$, assigned to a glass transition process associated with an enthalpy of 542.35 J/g , and extending from about $303\text{--}398\text{ K}$. It is probable that this broad peak includes another small one at 373 K due to the removal of some water trapped in the polymeric network. In the literature, several conflicting values of glass transition temperature (T_g) of PVP were found, ranging from 316 K at a scanning rate of 5 K/min to 450 K at a heating rate of 25 K/min . Several reasons are usually suggested for such confliction of T_g values including: presence of impurities, changes in specific heat involved, inability to attain near-equilibrium conditions during measurement and/or the faster rate of temperature change compared to the change in molecular rearrangement, along with the large influences of sorbed moisture due to the hygroscopic nature of the material. The minor endothermic peak at about 483 K in the thermograms of DSC for PVP may be attributed to a solid–solid transition of unspecific nature. Kumar et al reported a similar peak at 479 K . In addition to the endotherms at 345 and 483 K , the PVP sample showed an endothermic peak at about $T_{di} = 665\text{ K}$, which can be attributed to the thermal

chemical decomposition process associated with an enthalpy of 16.94 J/g.

On the other hand, FIG. 3 shows also the DSC thermograms for PVP/gelatin blend. One can observe that the addition of gelatin to PVP led to a shift of the peaks position for T_g and T_{d1} towards higher temperatures at about 363K and 683 K respectively. It is to be mentioned also that the peak at 483K for PVP disappeared in the thermogram of the blend.

Furthermore, FIG. 3 depicts the DSC curves for the PVP/gelatin doped with different concentrations of $MgCl_2$. It can be seen that the increase in doping

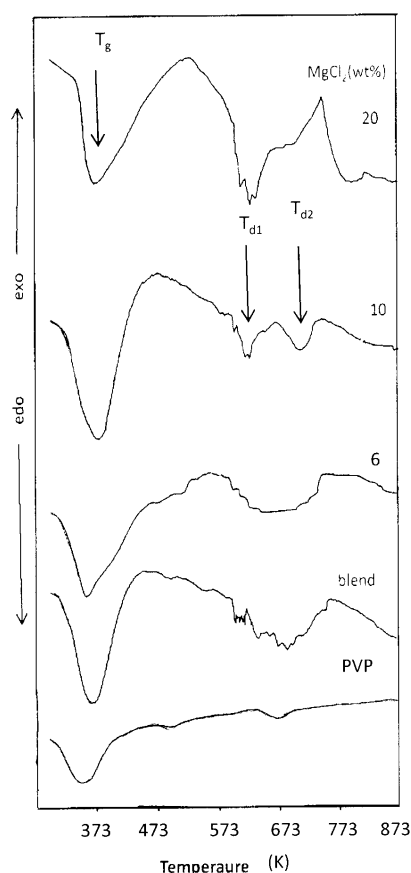


FIG. 3 DSC SCANS OF PURE PVP, PVP/GELATIN BLEND AND PVP/GELATIN BLEND DOPED WITH DIFFERENT COMPOSITIONS OF $MgCl_2$

concentration led to a shift of the T_g towards higher temperature, along with remarkable gradual increase of enthalpy values. The increase in the T_g values is due to the occurrence of grafting interactions of Mg^{2+} with amine group. Besides, the endothermic peak assigned to thermal decomposition of PVP at 665 K splits into two thermal decomposition temperatures (T_{d1} and T_{d2}) at about 665 and 783 K. These two peaks are probably of thermal decomposition nature associated to

different structures of polymeric matrix. This result is in agreement with that found in XRD analysis. As a result from pervious discussion, the increase of both $MgCl_2$ and gelatin into the polymeric matrix improved the thermal stability of the PVP.

UV/Vis optical absorption

FIG. 4 displays the UV-vis spectra of PVP/gelatin blend and blend doped with different content of $MgCl_2$. The spectra of undoped and doped blend had intense band at 208 nm, which may have been due to the presence of chromophoric group of gelatin. This result is in agreement with pervious reported. In addition the spectra exhibit a broad absorption band in between 245 and 285 nm. This band was assigned to the existence of carbonyl- groups associated with ethylene un-saturation $-(C=C)-C=O$. Moreover, the absorption spectra of the complexed films indicated an increase in the absorption intensity of the gelatin and shifting of the PVP broad band toward higher wavelength. The increase in the absorption intensity of gelatin and the shifting of the band of PVP with increasing $MgCl_2$ confirmed the complex formation between the polymer and the dopant.

The optical band gap (E_g) values were obtained from the absorption coefficient spectra according to the well-known energy exponential relation:

$$\alpha h\nu = B_{op} (h\nu - E_g)^m \quad (1)$$

where B_{op} is the film's constant, $h\nu$ is the photon energy, $\alpha = \frac{2.303 A}{d}$ is the absorption coefficient, A is

the absorbance, d is the film thickness and the exponent m depends on the kind of the optical transition that prevails, specifically, the n values are $\frac{1}{2}$, $\frac{3}{2}$, 2, and 3 for transitions directly allowed, directly forbidden, indirect allowed, direct forbidden, respectively.

Energy band gap values were obtained by extrapolating the straight line plot of $(\alpha h\nu)^{1/2}$ versus $h\nu$ as shown in FIG. 5. For the present study, the absorption relation $n = 2$, obtained by the best fit of eq. 1 indicated indirect allowed band transition. The linear dependence of the band gap on the dopant concentration is shown in FIG.6 with numerical equation:

$$E_g = -0.049 W + 5.31 \quad (2)$$

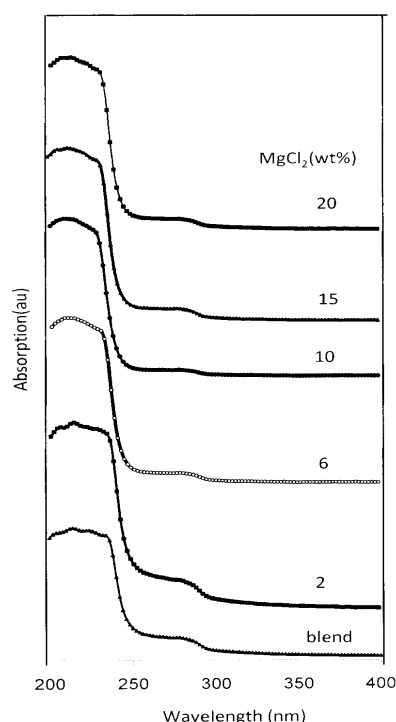


FIG. 4 DOPING LEVEL DEPENDENCES OF THE OPTICAL ENERGY GAP E_g (eV)

where W represents to the doping level. It is clear that, the monotonic decreasing in the values of the optical energy gap of PVP/gelatin blend with increasing the $MgCl_2$ content is observed. The change of E_g attributed to the change of induced energy states due to the change of intercalation mode. This confirmed the complex formation between the polymeric matrix and Mg^+ ions. On other wards, increasing $MgCl_2$ content may cause the localized states to overlap and extended in the mobility gap. This overlap may give us an evidence for decreasing energy gap when $MgCl_2$ content is increased in the polymeric matrix.

The Urbach tail was found to be related directly to similar exponential tail for the density of states of the band gap. The width of the Urbach tail is an indicator of defect levels in the forbidden gap. The following relation was used to calculate the width of the Urbach tail:

$$\alpha = \alpha_0 \exp\left(\frac{h\nu}{E_r}\right) \quad (3)$$

where α_0 is a constant and E_r is the width of the tail of the localized states due to the effect levels in the forbidden gap. The values of E_r are calculated from the slope of the linear dependence of the natural logarithm of the absorption coefficient versus the

photon energy (figure not shown). The doping level dependence of E_r is shown in FIG. 6. It is observed that the Urbach tail for pure blend is less than that for the doped ones, which increases with linear behavior as $MgCl_2$ content increase. The increase in E_r is due to the increase of the defects states in the polymeric matrix. The energy sum ($E_t = E_g + E_r$) can be taken to represent the mobility gap of the charge carriers existing in the conductivity specimens. The calculated values of E_r show decreasing with increasing dopant concentration indicating reduction of the charge trapping centers.

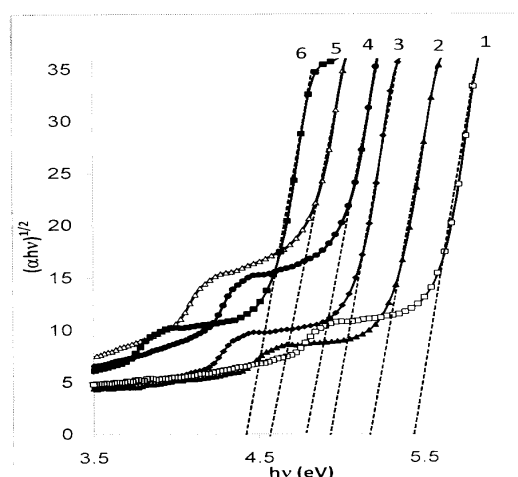


FIG. 5 THE ABSORPTION SPECTRA OF PVP/GELATIN BLEND AND PVP/GELATIN DOPED WITH $MgCl_2$

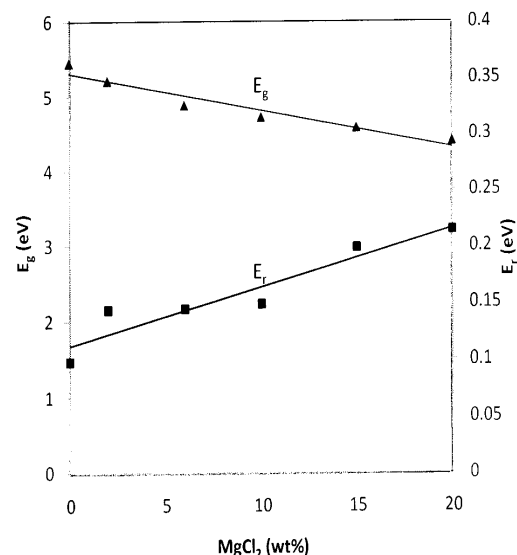


FIG. 6 DOPING LEVEL DEPENDENCE OF THE OPTICAL ENERGY GAP E_g (eV)

DC electrical resistivity

In polymeric films, the change of electrical resistivity (ρ) with temperature is due to the segmental motion,

which results an increase in the free volume of the system. This increase in free volume would facilitate the motion of ionic charge. Similar behavior was observed in a number of other films. The DC electrical resistivity of the polymer doped with metal halide mainly depends of the actual concentrations of the metal ions in the polymeric matrix and their mobility. The DC electrical resistivity values can be calculated from the following equation:

$$\rho = \frac{RS}{d} \quad (4)$$

where R is the resistance and S is the surface area of the electrode, and d is the thickness of the investigated sample.

Due to the presence of polarons and/or bipolaron, detected by the FT-IR analysis, the dc electrical resistivity (ρ) could be discussed on the basis of Kuivalainen et al modified inter-polaron hopping model. In this model the conduction mechanism could be interpreted on the basis of phonon-assisted charge carriers hopping between polaron and bipolaron bound states in the polymer. Thus the electrical resistivity is expressed as:

$$\rho = \frac{kT}{Ae^2 \gamma(T)^2} \frac{R_o^2 (y_p + y_{bp})^2}{\xi y_p y_{bp}} \exp\left(\frac{2BR_o}{\xi}\right) \quad (5)$$

where k is Boltzmann's constant, $A_1 = 0.45$; $B_1 = 1.39$; y_p and y_{bp} are the concentration of polarons and

bipolarons, respectively and $R_o = [3/(4\pi C_{imp})]^{1/3}$ is the typical separation between impurities whose concentration is C_{imp} ; $\zeta = (\zeta_{||} \zeta_{\perp}^2)^{1/3}$ is the average decay length of a polaron and bipolaron wave function; and $\zeta_{||}$ and ζ_{\perp} are the decay lengths parallel and perpendicular to the polymer chain, respectively. According to the calculations of Bredas et al, polarons and bipolarons induce defects of the same extension. The electronic transition rate between polaron and bipolaron states can be expressed as:

$$\gamma(T) = \gamma_o \left(\frac{T}{300 K} \right)^{11} \quad (6)$$

where the prefactor, $\gamma_o = 1.2 \times 10^{17} s^{-1}$, was estimated by Kivelson. The order of magnitude of q in the present work was adjusted with the impurity concentration C_{imp} , which actually was the fitting parameter. The parameter $\zeta_{||} = 1.06$ nm, while $\zeta_{\perp} \approx 0.22$ nm, which depends on the inter-chain resonance energy and the

inter-chain distance. Taking $y_p = y_{bp}$ for simplicity, which is an acceptable approximation and using equations (5) and (6), we can obtain the values of the hopping distance R_o . A linear temperature dependence of R_o for all doping levels is shown in FIG. 7. This indicates that the concentration of thermally activated polarons (acting as hopping sites for the charge carriers) increases gradually as the temperature increases. FIG.8 displays the dependence of hopping distance R_o on doping levels at $T = 370$ K. It can be seen that the hopping distance decreases with increasing $MgCl_2$. This may be related to a possible increase in the number of conduction paths created between the metal particles aggregates in the polymeric matrix in addition to a decrease in the width of the potential barriers within the conductivity regions. Therefore, more charge carriers may be able to hop by tunneling, resulting in the decrease in the resistivity.

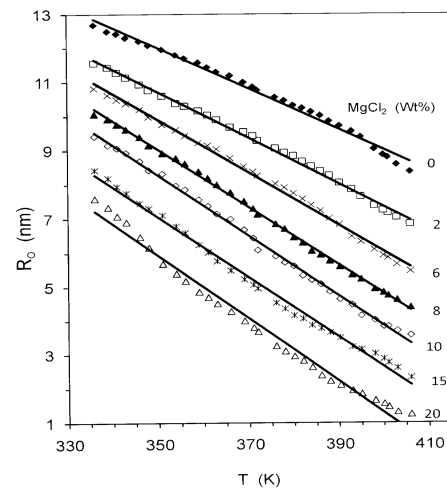


FIG. 7 TEMPERATURE DEPENDENCE OF HOPPING DISTANCE (R_o) FOR VARIOUS DOPED FILMS

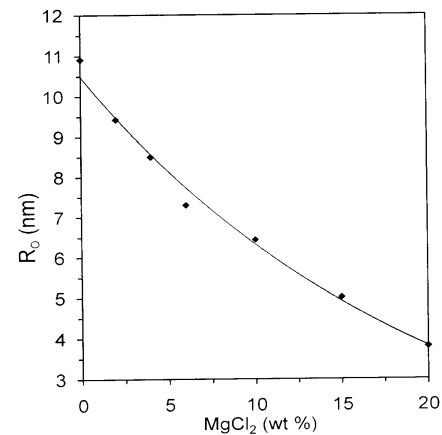


FIG. 8 DOPING LEVEL DEPENDENCE OF HOPPING DISTANCES R_o FOR VARIOUS DOPED FILMS AT $T = 370$ K

The DC electrical resistivity (ρ) was measured in the temperature range of 335-400 K for the PVP/gelatin blend treated with different contents of MgCl_2 . As Arrhenius relation the dependence of electrical resistivity (ρ) has the form:

$$\rho = \rho_0 \exp\left(\frac{-E_a}{kT}\right) \quad (7)$$

where ρ_0 is the proportionality constant, E_a is the thermal activation energy, and k is the Boltzmann constant. FIG.9 shows the temperature dependence of electrical resistivity of the complexes in the range 335-400 K. It is observed that as the temperature increases, the electric resistivity decreases for all complexes and this behavior is in agreement with the theory established by Armand et al. This can be rationalized by recognized the free volume model. When temperature is increased, the vibrational energy of a segment is sufficient to push against the hydrostatic pressure imposed by its neighboring atoms and create a small

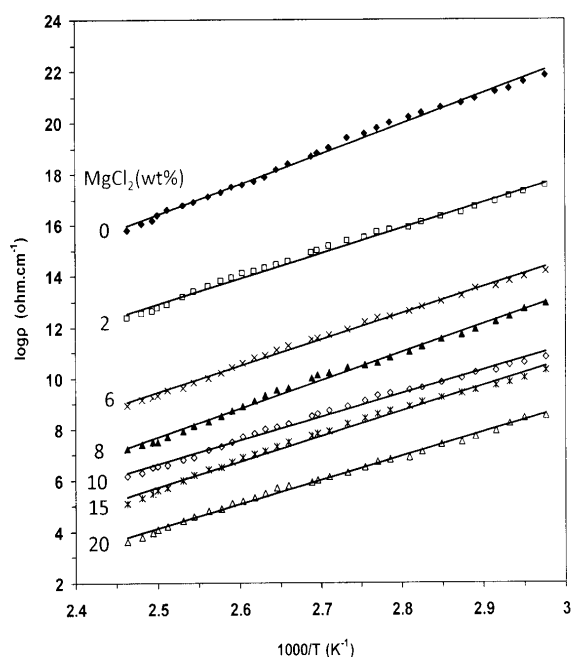


FIG. 9 TEMPERATURE DEPENDENCE OF THE LOGARITHM OF ELECTRICAL RESISTIVITY (ρ) FOR VARIOUS DOPED WITH DIFFERENT CONTENTS OF MgCl_2

amount of space surrounding its own volume in which around the polymer chain causes the mobility of ions and polymer segments and hence the electrical resistivity. Hence, the increment of temperature causes the decrease in electrical resistivity due to increased free volume and their respective ionic and segmental mobility.

The variation of logarithm of the electric resistivity (ρ) as a function of composition of MgCl_2 in PVP/gelatin blend at 370 K is shown in FIG. 10. It continued to decrease with increasing dopant concentration. The fast decrease in electric resistivity at lower dopant concentration of MgCl_2 is attributed to the formation of charge transfer complexes or decrease in the crystallinity of the blend, while the slow decrease at higher dopant concentrations is due to the formation of ionic aggregates.

The thermal activation energies were calculated from the slope of these plots, and the values are shown in FIG.10. These values are found to decrease with increasing concentration of MgCl_2 . This may be due to the fact that the addition of small amounts of dopant forms charge transfer complexes in the host lattice. These charge transfer complexes increase the electrical conductivity by providing additional charges in the lattice. This results in a decrease of activation energy. As a result both the electrical resistivity (ρ) and thermal activation energy (E_a) behaves nearly monotonically, this lead to important electrical technological applications.

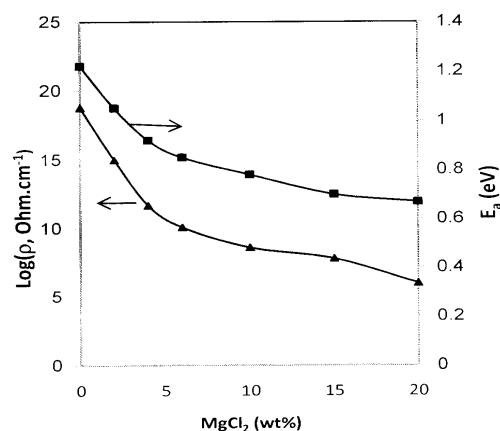


FIG.10 DOPING LEVEL DEPENDENCE OF HOPPING DISTANCES R_0 FOR VARIOUS DOPED FILMS AT $T = 370$ K

Conclusion

PVP/gelatin blend and its complexed films were prepared using a solvent casting technique. The XRD study reveals the amorphous nature of the blends and its complex films. Complex formation between the polymeric matrix and Mg ions was confirmed by both XRD and FT-IR analyses. DSC scans indicated that the thermal stability of the PVP is improved when blended with gelatin and loaded with MgCl_2 . Incorporation of magnesium chloride in PVP/gelatin blend increases the charge carriers, which causes a

decrease of both optical band gap and electrical resistivity of the prepared films. The decrease in optical band gap on doping levels was assigned to the formation of the charge transfer complex in the host lattice. The reduced values of the optical gaps improve their optical response. These films can be used as microwave sensors. The conductivity study indicates that the polymer blend can be effectively doped with MgCl_2 to improve its conductivity. The increase in conductivity is attributed to the formation of charge transfer complexes. The calculate optical band gap values of these materials as well as the magnitude of their electrical conductivities of the thin films suggest the possibility of considering them for use in the preparation of electronic devices.

REFERENCES

- Abd El-Kader F.H., Gafer S.A, Basha A. F., Bannan S.I. and Basha M.A.F., *J. Appl. Polym. Sci.*, 118 (2010): 413.
- Abdelaziz M., *J. Magn. Magn. Mater.* 2792 (2004): 184. Basha A.F. and Basha M.A.F., *Polym. Bull.* 68 (2012): 151.
- Bredas J.L., Chance R.R., Silbey R., *Phys. Rev. B* 26 (1982): 5843.
- Caykara T., Demirci S. and Kantoglu O., *Polym. Plast. Technol. Eng.* 46 (2007): 737.
- Chobagno M.B., Duclot J.M., Vashishta P., Mundy L.N. , and Shenoy G., *Fast-Ion Transport in Solid*, Noh-Holland, Amsterdam, (1979) 131.
- Davis E.A. and Mott N.F., *Philos. Mag.* 22 (1970): 903.
- Elasmawi I.S. and Adel Baieth H.E., *Cur. Appl. Phys.* 12 (2012) 141.
- Elimat Z.M., *J. Phys. D: Appl. Phys.* 39 (2006) 2824.
- Feng W., Tao H. and Liu Y., *J. Mater. Sci. Technol.*, 22 (2006): 230.
- Hatta F.F., Yahya M.Z.A. Ali A.M.M., Subban R.H.Y., Harun M.K. and Mohamed A.A., *Ionics* 11(2005): 418.
- Kaplan H. and Guner A., *J. Appl. Polym. Sci.* 78 (2000): 994-1001.
- Kivelson S., *Phys. Rev. B* 25 (1982) 3798.
- Kuivalainen P., Stubb H., Isotalo H., Yli P., Holmstrom C., *Phys. Rev. B* 31 (1985): 7900.
- Kumar V., Yang T. and Yang Y., *Int. J. Pharm.* 188 (1999): 221.
- Latour M., Anis K., Faria R.M., *J. Phys. D* 22 (1989): 806.
- Lokamatha K.M., Bharathi A., Kumar S.M.S. and Ramarao N., *Int. J. Pharm. Pharm. Sci.*, 2 (2010): 169.
- Mott N.F. and Gurney R.W., *Electronic*(1940) 34.
- Muthyala S., Bhonde R.R. and P.D. Nair, *Islets* 26 (2010) 357.
- Nagaahama H., Maeda H., Kashiki T., Jayakumar R., Furuike T. and Tamura H., *Carbohydrate Polym.* 79 (2009): 255.
- Rajendran S., Sivakumar M., Subadevi R., *Mater. Lett.*, 58 (2004): 641.
- Ravi M., Pavani Y., Kumar K.K., Bhvani S., Sharma A.K. and Rao V.V.R. N., *Mater. Chem. Phys.* 130 (2011): 442.
- Rosiak J., Burczak K., Olejniczak J. and Pekala W., *Polimery medycynie* 88 (1989): 4-8.
- Sengwa R. and Sankhla S., *Coll. Polym. Sci.* 285 (2007): 1237.
- Sessa D.J., Woods K.K., Mohamed A.A. and Palmquist D.E., *Ind. Crops Prod.* 33 (2011): 57.
- Sionkowska A., Kozłowska J. , Planecka A., Oanna J. and Wisnwska S., *Polym. Degrad. Stab.* 33(2008): 1.
- Sivaiah K., Rudramaddvi B.H. and Buddhudu S., *Indian J. Pure & Appl. Phys.* 48 (2010): 658.
- Sivaiah K. and Buddhudu S., *Indian J. Pure & Appl. Phys.*, 49 (2011): 377.
- Subba V., Han X., Zhu Q.Y. and Qiang L., *Microelectr. Engin.* 8 (2006): 281-288.
- Umadevi C., Mohan K.R., Achari V.B.S., and Sharma A.K., *Ionics* 16 (2010): 751.
- Urbach F., *Phy. Rev.*, 92 (1953): 1324.